Quantum Electronics **42** (2) 170 – 174 (2012)

LASER TECHNOLOGIES

PACS numbers: 42.62.Cf; 52.38.Mf; 83.60.Np
DOI: 10.1070/QE2012v042n02ABEH014709

Influence of an electric field on near-surface processes in laser processing of metals

S.V. Vasil'ev, A.Yu. Ivanov

Abstract. **It is shown that by varying the external electric field with different polarity from 0 to 10^6 V m^{-1} in the course of laser processing with the mean radiation flux density ~10^6 W cm^{-2} the change in the evolution features of the plasma torch at the surface of some metals (Cu, Al, Sn, Pb) at early stages is quantitative rather than qualitative. At the same time the characteristic size of the target material droplets, carried out from the irradiated zone, becomes essentially (by several times) smaller as the amplitude of the external electric field strength grows, independently of its polarity.**

Keywords: *laser radiation, electric field, plasma formation, gravity-capillary waves.*

1. Introduction

In connection with permanent expansion of the field of technological applications of lasers new problems arise, the solution of which requires investigation of processes taking place under the action of light fluxes on the surface of solids. Such studies are of particular importance for choosing the most efficient regimes of laser processing of materials, including laser pattern cutting, perforation, welding of materials, modifying their surface properties, and laser film deposition, as well as for developing new methods for control of laser technological processes. In addition, such studies are of separate scientific interest. It is urgent to study the mechanisms of changing the surface relief of a solid in the course of exposing it to pulsed laser radiation under different external conditions, particularly, in the presence of external electric fields.

The study of processes that occur in a vapour-plasma cloud arising near the surface of the irradiated sample are also of great interest since they affect most significantly the material processing [1 – 5].

The aim of the present paper is to study the influence of electric fields of different strength (from 0 to 10^6 V m^{-1}) on the spatial and temporal evolution of the laser plasma arising under the action of millisecond laser pulses at the surface of metals (copper, aluminium, tin, lead) and on the mechanisms of formation of the surface relief of the irradiated samples.

S.V. Vasil'ev, A.Yu. Ivanov Yanka Kupala Grodno State University, ul. Ozheshko 22, 230023 Grodno, Belarus; e-mail: serg.vas@tut.by, ion_ne@mail.ru

Received 22 August 2011; revision received 15 November 2011
Kvantovaya Elektronika **42** (2) 170 – 174 (2012)
Translated by V.L. Derbov

2. Experimental

The scheme of the experimental setup used in the study is presented in Fig. 1. The radiation of the GOR-100M ruby laser (*1*) (λ = 0.694 μm) operating in the free oscillation regime (pulse duration ~1.2 ms, Fig. 2) passed through the focusing system (*2*) and was directed through the hole in the electrode (*3*) onto the sample (*4*) that served as the second electrode and was mounted in air at a pressure of 10^5 Pa. The radiation spot diameter on the sample with sharp edges was varied in the course of the experiments from 1 to 2 mm.

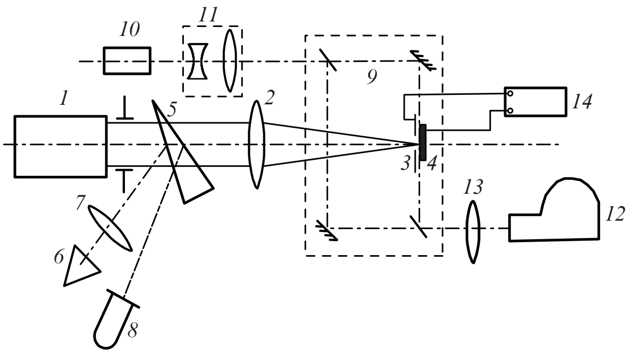

Figure 1. Schematic diagram of the experimental setup.

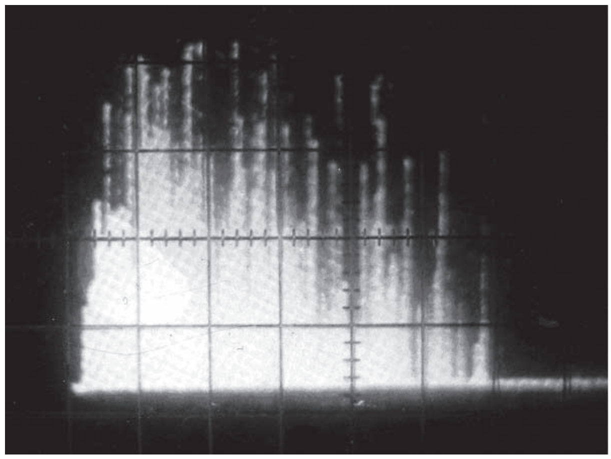

Figure 2. Oscillogram of the radiation pulse from the GOR-100M laser. The scanning rate is 200 μs div.$^{-1}$.

From the front face of the glass wedge (*5*) a part (4%) of laser radiation was directed into the IMO-2N energy meter (*6*), whose entrance window was located in the focal plane of the lens (*7*). The energy of the laser pulses varied from 5 to 60 J. The FEK-14 coaxial photodetector (*8*), the signal from which was coupled to the S8-13 oscilloscope, was used to record the temporal shape of the laser pulse. The voltage was applied to the electrodes (*3*, *4*) from the source (*14*), built on the basis of the UN 9/27-13 voltage multiplier of the TVS-110 unit. The source allowed the voltage variation within 25 kV and its stabilisation in the course of the experiment.

To study the spatial and temporal evolution of the laser plasma torch in the course of laser radiation action on the sample, we used the method of high-speed holographic motion-picture recording [6]. The interelectrode gap was placed in one of the arms of a Mach–Zehnder interferometer (*9*), which was illuminated with the radiation of the ruby laser (*10*) (λ = 0.694 μm) operating in the free oscillation regime. The pulse duration of the radiation amounted to ~400 μs. The transverse mode selection in the probing laser was accomplished using the aperture, placed in the cavity, and the longitudinal mode selection was provided by the Fabry–Perot cavity standard used as the output mirror. The probing radiation after the collimator (*11*) was a parallel light beam with the diameter up to 3 cm, which allowed observation of the vapour-plasma cloud development.

The interferometer was attached to the SFR-1M high-speed recording camera (*12*), in which the plane of the film was conjugate with the meridian section of the laser beam, acting on the sample, by means of the objective (*13*). The high-speed camera operated in the time magnifier regime. The described setup allowed recording of time-resolved holograms of the focused image of the laser plasma torch. Separate holographic frames provided temporal resolution no worse than 0.8 μs (the single frame exposure time) and the spatial resolution in the object field ~50 μm. The diffraction efficiency of the holograms allowed one to reconstruct and record interference and shadow pictures of the studied process under the stationary conditions.

To study the surface shape of the crater that appears on the plate, we used the fringe projection method [7], which in the present case appeared to be more efficient than holographic methods of surface relief imaging and the stereophotogrammetric method [8], since, already at the stage of fringe projecting, it allowed obtaining a picture with controllable sensitivity of measurements and sufficiently good visibility of fringes, controlled visually. The sensitivity of measurements (relative fringe displacement) was set by changing the period of the projected fringes, and the good visibility was provided by changing the angle of illumination of the studied surface till removing the light flares from the crater surface. The present method is thoroughly described and successfully used in [9–11].

3. Experimental results and discussion

The experimental results have shown that at any polarity of the applied voltage [with positive or negative potential at the irradiated sample with respect to the electrode (*3*)] the topography of the crater is practically identical and is determined by the energy distribution over the focusing spot of the laser radiation (Figs 3, 4).

Figures 5a–c display the interferograms, reconstructed from the holograms recorded at different instants in the course of high-speed holographic motion-picture shooting. The figure clearly illustrates both the initial stage of the laser torch development and the plasma flow around the electrode (*3*) at different directions of the external electric field strength vector.

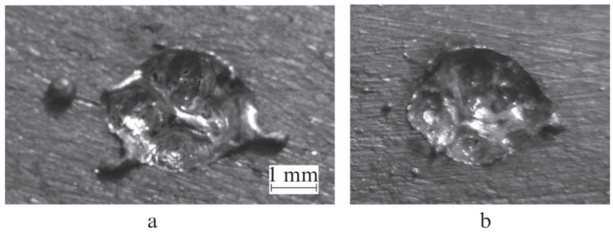

Figure 3. Photographs of the craters obtained under the action of laser pulses on the target in the absence of the external electric field (a) and in the presence of the field (b).

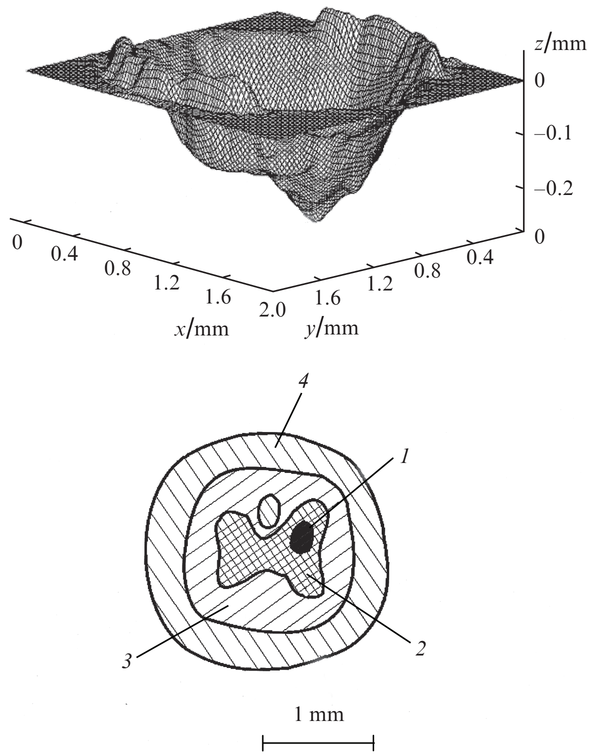

Figure 4. Volume topogram of a crater (a) and the distribution of light energy density over the transverse cross-section of the laser beam (b): 4.5 (*1*), 3.5 (*2*), 1.2 (*3*), and 0.8 J mm^{-2} (*4*).

Figures 5d–f represent the data on the distribution of concentration of free electrons in the plasma of an evaporated metal at different instants, obtained by processing the interferograms [12]. Although the energy distribution over the laser radiation focusing spot is not uniform, the lines of equal concentration are practically smooth, which is an evidence of relatively uniform ionisation of the eroded substance vapours. It is essential that, despite a substantial increase in the plasma formation over time, the mean electron concentration in the torch remains practically unchanged and even slightly grows, which may be associated both with a constant increase in the mass of emitted substance and with secondary ionisation of the plasma by the laser radiation. Note, that the presence of an external electric field weakly affects the concentration of electrons in the laser plasma torch.

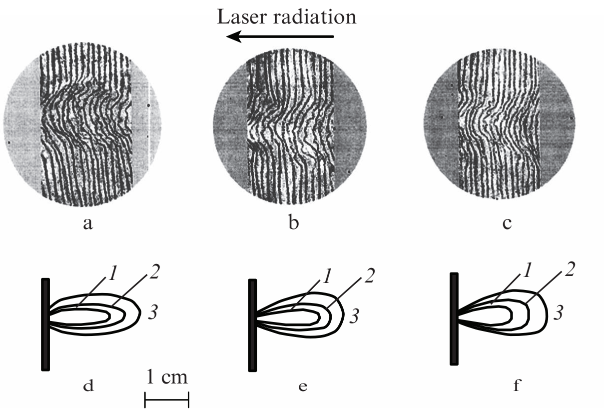

Figure 5. Interferograms of laser plasma torches (a, b, c) and electron concentration isolines in them (d, e, f) at the negative target potential (b, e) and at the positive target potential (c, f) at the instants 72 μs after the onset of the laser action; curve (*1*) corresponds to the electron concentration 5×10^{18}, curve (*2*) to 2.5×10^{18}, and curve (*3*) to 10^{18} cm^{-3}.

When the interelectrode separation was 2 cm, the maximal transverse size of the vapour-plasma cloud at the surface of the electrode (*3*) for negative voltage on the target was 2 cm and in the absence of the external electric field it was 1.5 cm. This may be observed both in the interferograms and by the burn on the polyethylene film protecting the second electrode. As seen from interferograms, after reaching the second electrode in 56, 64, and 72 μs, respectively, the vapour-plasma cloud practically does not grow in the transverse dimensions. Probably it is due to the flowing out of the plasma from the interelectrode gap through the hole in the electrode (*3*), which is used for passing the laser radiation to the target (the hole diameter being 1 cm).

Figure 6 presents the time dependences of the plasma torch front motion velocity at different directions of the external electric field strength vector, calculated by using the information, obtained by analysing the temporal variation of the interferograms. It is seen that even when the plasma front reaches the electrode (*3*), its velocity not only does not decrease (which is typical for late stages of the laser plasma torch existence [6]), but even increases; this happens both in the presence of the external electric field of any orientation and in the absence of the field. As already mentioned, this is due to the permanent and significant increase in the mass of the material, carried out under the action of laser radiation on the irradiated sample, as well as to the secondary ionisation of plasma by laser radiation.

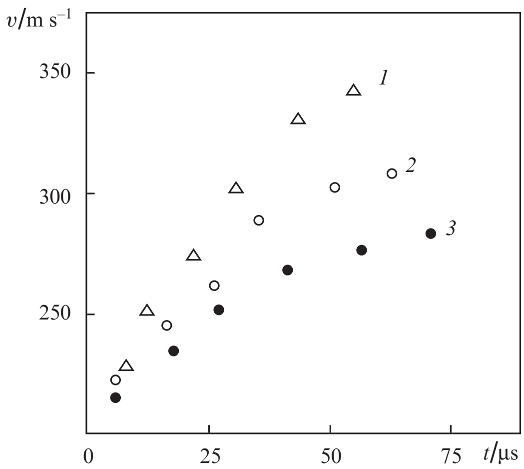

Figure 6. Time dependences of the velocity of the plasma torch front motion at the negative target potential (*1*), in the absence of the field (*2*), and at the positive target potential (*3*).

The maximal expansion velocity of the plasma torch amounted to 350 m s^{-1} for the negative voltage at the target, 310 m s^{-1} in the absence of the external electric field, and 270 m s^{-1} for the positive voltage applied to the target.

When either positive or negative potential is applied to the sample, many small droplets appear on its surface after the laser action (Figs 3 and 7). In particular, at the laser pulse energy 20 J, the diameter of the focusing spot 2 mm, and the electric field strength 10^6 V cm^{-1} we observed ejection of droplets having the mean characteristic size less than 0.1 mm to the distance up to 2 cm from the crater centre. The maximal characteristic size of the droplets was ~0.4 mm.

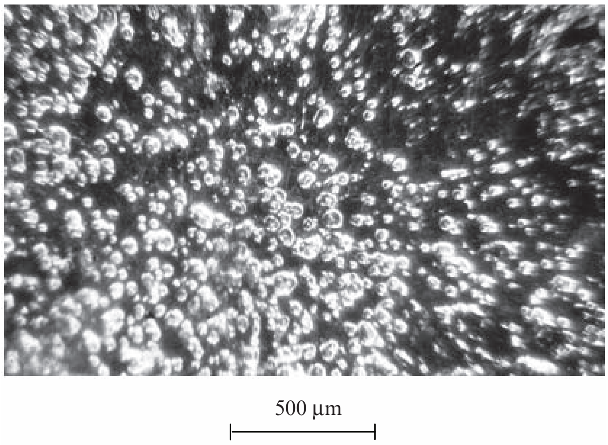

Figure 7. Photographs of the microscopic surface relief of the crater outer zone.

In the absence of the external electric field the mean size of the droplets was ~0.4 mm. The droplets were seen at the distance up to ~1 cm from the crater centre.

In accordance with the results presented above, the dynamics of the processes on the surface of a sample, placed in an external electric field with the strength from 0 to 10^6 V m^{-1} and subject to the action of the pulsed laser radiation with the parameters mentioned above, is thought to be the following. The primary plasma formation and the initial stage of the laser torch development, in principle, do not differ from those observed in the absence of the external electric field. The metal is melted and evaporated. As a result of local formation of vapour and plasma [13–16], the erosion torch begins to form with the fine-dispersed liquid-drop phase. Note, that the bulk evaporation is promoted by the gases, diluted in the metal, and by the spatiotemporal nonuniformity of the laser radiation [15]. At a radiation flux density 10^6-10^7 W cm^{-2} the bulk evaporation is typical of all metals used in the experiments [16]. Obviously, the presence of the external electric field affects (increases or decreases depending on the direction of the field strength vector) the velocity of motion of the plasma front and causes some distortion of the plasma cloud shape. It is essential that the mentioned differences (at the considered parameters of laser radiation) are observed only at the initial stage of the laser torch development, because after the vapour-plasma cloud reaches the electrode (*3*) an electric breakdown (short-circuit) occurs, and the external field in the interelectrode gap disappears.

Consider now the motion of the molten metal droplets in the vapour-plasma cloud. In our opinion, the significant difference in the characteristic size of droplets, observed on the surface of the irradiated sample in the presence of the external electric field (independent of the direction of the field strength vector) and in the absence of the field, is a manifestation of the following mechanism of droplet formation [17, 18]. It is known that at the surface of a liquid (including a liquid metal) the formation of gravity-capillary waves [17–20] is possible under the action of various perturbations. Undoubtedly, the examples of such perturbations are the spatially nonuniform evaporation of the target material due to nonuniform heating caused by nonuniform energy distribution over the focusing spot [10], the nonuniform primary plasma formation [18, 21–24] caused by roughness of the irradiated sample surface [10], and, in the first place, the slop of the molten metal initiated by each spike of laser radiation, acting on the exposed sample [11].

Using the method presented in [19], one can show that at insignificant thickness of the molten metal layer [confirmed by the view of the 'outer' (directed) zone of the crater, particularly, the absence of fillets of significant height at the crater edge] the dispersion equation for the gravity-capillary waves takes the form [17]

$$\omega^2 = \frac{\alpha k^3}{\rho} + gk - \frac{kE_0E'}{4\pi\rho\xi'}\Big|_{z=0}, \quad (1)$$

where α is the surface tension coefficient of the molten metal; ρ is the metal density; g is the free fall acceleration; k is the magnitude of the wave vector of the gravity-capillary wave; E_0 is the electric field strength at the surface ($z = 0$) of the molten metal (the z axis is perpendicular to the surface of the irradiated sample, directed towards the laser radiation source and parallel to the vector $\boldsymbol{E}_0$); $E' = -\partial\varphi'/\partial z$ is the perturbation of the electric field in the space surrounding the molten metal; ξ' is the small displacement of the surface of the liquid in the z axis direction in the gravity-capillary wave.

Because for the uniform field E_0 the potential is $\varphi = -E_0 z$ (the potential at the metal surface is considered to be zero), the displacement of the mentioned surface by the small quantity ξ' leads to a small distortion of the potential:

$$\varphi'\big|_{z=0} = E_0\xi'. \quad (2)$$

It follows from Fig. 3 that the maximal concentration of electrons in the plasma formation does not exceed $\sim 10^{18}$ cm^{-3}, which corresponds to the change in the dielectric constant of the medium ε by approximately 10^{-5}. Therefore, near the metal surface $\varepsilon \cong 1$ and with the boundary condition (2) taken into account

$$\varphi' = E_0\xi' \mathrm{e}^{-kz}.$$

In this case, the dispersion equation for gravity-capillary waves takes the form

$$\omega^2 = \frac{\alpha k^3}{\rho} + gk - \frac{k^2E_0^2}{4\pi\rho}.$$

Because the frequency of the gravity-capillary waves ω is determined by the temporal characteristics of the abovementioned perturbations and, therefore, does not depend on the strength of the electric field E_0, the growth of the magnitude E_0 (independent of the direction of the vector $\boldsymbol{E}_0$) should cause the increase in the magnitude of the wave vector $k = 2\pi/\Lambda$ and the decrease in the wavelength Λ of the gravity-capillary wave. If we assume that the droplets are 'torn away' by the plasma flow from the 'tops' of the gravity-capillary wave and, therefore, their characteristic size is proportional to Λ, then it becomes clear why in the presence of the external electric field (of any direction) the observed mean size of the droplets becomes essentially reduced.

The escaped droplets possess the charge of the same sign as the sample. That is why the droplets begin to move with acceleration towards the second electrode. However, since the maximal initial velocity of the outgoing droplets under the analogous conditions [10] is $\sim$45 m s^{-1}, i.e., an order of magnitude smaller than the velocity of vapour-plasma cloud spreading, the droplets do not reach the electrode (*3*) before the moment of the breakdown in the interelectrode gap. In what follows (in the absence of the external electric field) the droplets move under the action of the same forces as in [10] and, therefore, in the way, described in [10]. In this case, having acquired at the stage of accelerated motion in the electric field the velocity, exceeding the initial one, the droplets may fly to a greater distance along the surface of the irradiated sample than in the absence of the electric field, which is observed in the experiment. Moreover, having moved to a greater distance from the sample surface and, therefore, being affected by the plasma for longer time before returning to the surface, the droplets may be split into finer parts than in the absence of the external field.

It should be noted that the droplets in the erosion torch may appear not only due to the molten pool surface instability, but also due to the condensation of the vapours of the erosion products [25, 26]. Moreover, since the droplets produced in the course of condensation of vapours may be charged [27], they, similar to those carried out from the molten pool, in the electric field may be removed from the crater to a greater distance than in the absence of the electric filed. However, this mechanism of plasma formation is dominating under somewhat different conditions of laser radiation acting on the material [25–28], namely, at significantly greater mean radiation flux density (10^8–10^9 W cm^{-2}) and smaller exposure duration (single pulses of laser radiation were used with the duration 100–200 ns and with less smooth temporary shape). In the case of such a regime of laser metal processing one observes the screening of the irradiated sample by the plasma cloud, which is possible only at the concentration of the ablated material vapour essentially exceeding 10^{18} cm^{-3} (see Fig. 5). In this case, one observes intense formation of droplets with the dimension $\sim$200 nm and smaller, and this process is most active at the late stages of laser radiation action on the material (at decreasing intensity of laser action) [28] and even after its termination [25]. At smaller radiation flux density, characteristic of the experiment considered in the present paper ($\sim 10^{18}$ cm^{-3}), the condensation of droplets from the vapour of ablation products is expected to be less intense. Therefore, the essential contribution of the condensation mechanism to the process of formation of large drops (having the size 0.1–0.4 mm, see Figs 2 and 7), especially at early stages of the process, i.e., before filling the entire interelectrode gap by the plasma cloud, seems to be hardly probable.

4. Conclusions

The studies performed have shown that under the action of laser radiation with the mean radiation flux density ~10^6 W cm^{-2} at the surface of some metals (Cu, Al, Sn, Pb) in the external electric field with different polarity and the strength up to 10^6 V m^{-1} the characteristic size of the target substance droplets, carried out of the irradiated zone, decreases by several times with increasing external electric field strength. Probably, this is due to a change in the wavelength of the gravity-capillary wave, excited on the molten metal surface. The observed effect offers the possibility to control the size of the metallic droplets in the course of laser deposition of thin films.

References

1. Anisimov S.I., Imas Ya.A., Romanov G.S., Khodyko Yu.V. *Deystvie izluchenii bol'shoy moschnosti na metally* (Action of High-Power Radiation on Metals) (Moscow: Nauka, 1970).
2. Vedenov A.A., Gladush G.G. *Fizicheskiye protsessy pri lasernoy obrabotke metallov* (Physical Processes in Laser Processing of Materials) (Moscow: Energoatomizdat, 1985).
3. Prokhorov A.M., Konov V.I., Ursu I., Mikhalesku I.N. *Vzaimodeystvie lazernogo izlucheniya s metallami* (Interaction of Laser Radiation with Metals) (Moscow: Nauka, 1982).
4. Ready J.F. *Industrial Applications of Lasers* (New York: Academic, 1997)
5. Arutyunyan R.V., Baranov V.Yu., Bol'shov V.A., et al. *Vozdeystvie lasernogo izlucheniya na materialy* (Action of Laser Radiation on Materials) (Moscow: Nauka, 1989).
6. Barikhin B.A., Ivanov A.Yu., Nedolugov V.I. *Kvantovaya Elektron.*, **17**, 1477 (1990) [*Sov. J. Quantum Electron.*, **20**, 1386 (1990)].
7. West C.M. *Holographic Interferometry* (New York: John Wiley & Sons, 1979).
8. Caulfield H.J. (Ed.) *Handbook of Optical Holography* (New York: Academic Press, 1979).
9. Vasil'ev S.V., Ivanov A.Yu., Lyalikov A.M. *Kvantovaya Elektron.*, **20**, 616 (1993) [*Quantum Elelctron.*, **23**, 535 (1993)].
10. Vasil'ev S.V., Ivanov A.Yu., Lyalikov A.M. *Kvantovaya Elektron.*, **22**, 830 (1995) [*Quantum Elelctron.*, **25**, 799 (1995)].
11. Bosak N.A., Vasil'ev S.V., Ivanov A.Yu., Min'ko L.Ya., Nedolugov V.I., Chumakov A.N. *Kvantovaya Elektron.*, **27**, 69 (1999) [*Quantum Elelctron.*, **29**, 69 (1999)].
12. Ostrovskii Yu.I., Butusov M.M., Ostrovskaya G.V. *Golograficheskaya interferometriya* (Holographic Interferometry) (Moscow: Nauka, 1977).
13. Yel'yashevich M.A., Min'ko L.Ya., Romanov G.S., Stankevich Yu.A., Chivel' Yu.A., Chumakov A.N. *Izv. Akad. Nauk SSSR. Ser. Fiz.*, **49**, 1132 (1985).
14. Goncharov V.K. *Inzhenerno-fizicheskii zhurnal*, **62**, 665 (1992) [*Journal of Engineering Physics and Thermophysics*, **62**, 472 (1992)].
15. Goncharov V.K., Kontsovoy V.L., Puzyrev M.V. *Inzhenerno-fizicheskii zhurnal,* **66**, 662 (1994) [*Journal of Engineering Physics and Thermophysics*, **66**, 588 (1994)].
16. Goncharov V.K., Kontsevoy V.L., Puzyrev M.V. *Kvantovaya Elektron.*, **22**, 249 (1995) [*Quantum Elelctron.*, **25**, 232 (1995)].
17. Vladimirov V.V., Golovinskii P.M. *Zh. Eksp. Teor. Fiz.*, **82**, 1464 (1982) [*Sov. Phys. JETP*, **55**, 848 (1982)].
18. Zaykin A.E., Levin A.V., Petrov A.L., Stranin S.A. *Kvantovaya Elektron.*, **18**, 708 (1991) [*Sov. J. Quantum Elelctron.*, **21**, 643 (1991)].
19. Rabinovich M.I., Trubetskov D.I. *Vvedenie v teoriyu kolebanii i voln* (Introduction to the Theory of Oscillations and Waves) (Moscow: Nauka, 1984).
20. Zaykin A.E., Levin A.V., Petrov A.L. *Kvantovaya Elektron.*, **21**, 486 (1994) [*Quantum Elelctron.*, **24**, 449 (1994)].
21. Dorofeev I.A., Libenson M.N. *Opt. Spektrosk.*, **76**, 73 (1994) [*Opt. Spectrosc.*, **76**, 66 (1994)].
22. Golub' A.P. et al. *Zh. Tekh. Fiz.*, **51**, 316 (1981) [*Sov. Phys. Tech. Phys.*, **26**, 191 (1981)].
23. Datskevich N.P. et al. *Kvantovaya Elektron.*, **11**, 853 (1984) [*Sov. J. Quantum Electron.*, **14**, 579 (1984)].
24. Chumakov A.N. et al. *Kvantovaya Elektron.*, **21**, 773 (1994) [*Quantum Electron.*, **24**, 718 (1994)].
25. Goncharov V.K., Kozadayev K.V. *Inzhenerno-fizicheskii zhurnal*, **83**, 80 (2010) [*Journal of Engineering Physics and Thermophysics*, **83**, 90 (2010)].
26. Chumakov A.N., Bereza N.A., Hu Dz.D., Bosak N.A., Guo Z.H., Hie K.K. *Inzhenerno-fizicheskii zhurnal*, **84**, 524 (2011) [*Journal of Engineering Physics and Thermophysics*, **84**, 567 (2011)].
27. Klimentov S.M. et al. *Laser Phys.*, **8** (6), 1 (2008).
28. Goncharov V.K., Kozadayev K.V., Shchegrikovich D.V. *Inzhenerno-fizicheskii zhurnal*, **84**, 781 (2011) [*Journal of Engineering Physics and Thermophysics*, **84**, (2011)].